



The 1st International Joint Mini-Symposium on Advanced Coatings between Indiana University-Purdue University Indianapolis and Changwon National University

## Development of A New Coating System for The High Functional Mold in Thin-wall Casting

Eun-Hee Kim, Yeon-Gil Jung\*, Je-Hyun Lee

*School of Advanced Materials Science and Engineering, Changwon National University, Changwon, Gyeongnam 641-773, Republic of Korea*

---

### Abstract

A new inorganic binder system has been developed to prepare the mold having a high strength for the thin-walled casting. To increase the fracture strength at high temperature, a large amount of inorganic binder should be converted into glass phase and the generated glass phase has to be homogeneously coated on the surface of starting particles. In this work, two types of process were employed to investigate the coating and glassification efficiencies of inorganic precursor. In the first process (process I), the green body consisting of starting powder and organic binder was dipped in the inorganic precursor solution. In the second process (process II), the starting powder was coated by inorganic precursor, and then the organic binder was used to form the green body. The mold sample prepared using process II showed the higher strength value than that using process I, owing to the increment effect on the glassification efficiency by the loss of inorganic precursor in process I. The prepared real mold was perfectly produced and the casted product showed a clean surface without defects such as dross, nonmetallic inclusions, and crack. Consequently, the new inorganic binder system could be applied for preparing the mold for the thin-wall casting having high mechanical properties.

© 2014 The Authors. Published by Elsevier Ltd. This is an open access article under the CC BY-NC-ND license (<http://creativecommons.org/licenses/by-nc-nd/3.0/>).

Selection and Peer-review under responsibility of the Chairs of The 1st International Joint Mini-Symposium on Advanced Coatings between Indiana University-Purdue University Indianapolis and Changwon National University, Indianapolis.

*Keywords:* Sol-gel processes; Inorganic precursors; Mechanical properties; Glassification; Coating process.

---

---

\* Corresponding author. Tel.: +82-55-213-3710; fax: +82-55-262-6486.  
E-mail address: [jungyg@changwo.ac.kr](mailto:jungyg@changwo.ac.kr)

## 1. Introduction

Recently, in precision casting, the ceramic mold using inorganic binders such as ethyl silicate and colloidal silica aquasols has been developed, especially applicable to the precision casting using a lost wax casting technique [1,2]. Saridikmen et al. studied the ceramic mold using inorganic binders with two different compositions, ethyl silicate and ethyl silicate/aluminum tri-sec-butoxide solution [3]. However, the reaction between ceramic mold and molten metal generated during the casting as well as the high temperature of molten metal (above 1450 °C) and the high shrinkage of ceramic mold has lots of limiting factors to be applied to real work environments. Jiang et al. researched the dimensional changes and variability of ceramic molds in steel castings through a stepped pyramid-shaped part [4]. In the ceramic mold process using silicate as inorganic binder, the addition of gelling agent such as ammonium carbonate and acetic acid is essential. However, the molds fabricated by the convert mold process have many advantages for precision casting, such as without gelling agent, high strength, enhancement of collapse, easy processability, and high thermal stability, making it useful in fabricating components of automobile and aircraft. Conventionally, the thin-wall casting of complex shape with the thickness of 5 mm or less should be performed using a precision casting process. However, it leads to a variety of difficulties of rising production costs and lower productivity, and so on. Therefore, the convert mold process has been applied into the sand mold in the thin-wall and precision casting. Typically, the convert mold process is divided into five main processes: (1) forming the starting mold coated with an organic binder, (2) dipping the coated mold into a slurry with inorganic precursors, (3) first drying for 1 h at 80 °C, (4) second drying for 1 h at 200 °C, and (5) heat-treating for 1 h at 1000 °C, resulting in the conversion of the organic-coated mold to the inorganic-coated mold

The reaction mechanisms of the inorganic precursors used in the convert mold process are as follows [5,6]:

Sol–gel reaction:



Hydrolysis reaction:



Heat treatment:



where  $\text{Si(OEt)}_4$ ,  $\text{Si(OH)}_4$ ,  $\text{EtOH}$ ,  $\text{SiO}_2$ ,  $\text{NaOMe}$ ,  $\text{NaOH}$ , and  $\text{MeOH}$  denote TEOS, silanol, ethyl alcohol, silica, sodium methoxide, sodium hydroxide, and methyl alcohol, respectively [7]. TEOS is degraded to silanol and ethyl alcohol through the hydrolysis reaction (Eq. (1)), and silica is subsequently formed by the condensation reaction between many silanol molecules (Eq. (2)). These two reactions are usually called a sol–gel reaction.  $\text{NaOMe}$  is hydrolyzed to form  $\text{NaOH}$  (Eq. (3)). The synthesized sodium hydroxide and silica is converted into sodium silicate ( $\text{Na}_2\text{O} \cdot \text{SiO}_2$ ) at the temperature of about 1000 °C, calls as glassification. Sodium oxide ( $\text{Na}_2\text{O}$ ) as network modifier is added to allow easy formation of a glass phase and to decrease the viscosity of the glass phase [8]. Consequently, the organic binder coated on the mold is converted into the inorganic binder by the reactions shown in Eqs. (1)–(4). Namely, the liquid-phase precursor is converted to a solid-phase glass by the sol–gel reaction and heat treatment, subsequently inducing the mechanical and thermal properties of the mold [9]. Therefore, the generated glass phase must be homogeneously formed on the interfaces and surfaces of starting particles in the mold as well the coating and glassification efficiencies of inorganic binder precursors into the glass phase should be increased. Our early works were researched about the use of a new inorganic precursor and the development of a new process to prepare the mold with high strength of mold for thin-wall casting. The new inorganic precursor without the sol-gel reaction instead of the inorganic binder used in the conventional convert mold process has been applied [10], and the new processes which is called an in situ process, has been introduced [11]. Even though the convert mold process reveals the improved mold collapsibility and thermal stability, the hydrolysis reaction in the inorganic precursor induces that the atmospheric moisture should be controlled during the process. Therefore, in our works, molds for thin-wall casting were fabricated using two types of binder system, tetraethyl orthosilicate (TEOS) with the hydrolysis

reaction and polydimethyl siloxane (PDMS) without the hydrolysis reaction as silica ( $\text{SiO}_2$ ) precursors and sodium methoxide (NaOMe) as a precursor of  $\text{Na}_2\text{O}$ . These were studied as functions of dipping time and binder composition in an effort to enhance the fracture strength, achieve a more favorable collapsibility, and improve the thermal and dimensional stability. In addition, in the convert mold process, an inorganic precursor is generally coated on the organic binder which is used to fix the mold shape. This inorganic precursor is easily lost by burning of the organic binder with a low decomposition temperature during the heat treatment, resulting in a reduction in the glassification efficiency of inorganic precursor. Therefore, inorganic precursor was coated on the starting particles prior to the organic binder. It causes the homogeneous coating of the inorganic precursor on the surfaces of particles and excellent conversion of the inorganic precursor into the glass phase. In this paper, a new process for enhancing the coating effect and glassification of inorganic precursor is introduced. Namely, the inorganic precursor was coated on the starting powder preparatory to the organic binder, and then the organic binder was added to form the mold. In addition, the new coating process for the mold preparation with high glassification efficiency was divided into two processes: in the first process, individual inorganic precursors were independently coated on the starting particles through the continuous coating process, and in the second process, the mixed inorganic precursor was coated on the starting particles. The coating morphology and surface microstructure of the powders and molds prepared by the new coating processes and inorganic precursor were compared with those by the conventional convert mold process, using various analytical techniques. The relationship between fracture strength, and coating process and binder composition were discussed based on the microstructures observed before and after heat treatment.

## 2. Experimental procedure

### 2.1. A new inorganic binder system

The inorganic binder systems for thin-wall casting were prepared using TEOS (Sigma–Aldrich Korea, Yongin, Korea) of silicate type and PDMS (Sigma–Aldrich Korea, Yongin, Korea) of siloxane type as the  $\text{SiO}_2$  precursors, and NaOMe (Sigma–Aldrich Korea, Yongin, Korea) as the sodium oxide ( $\text{Na}_2\text{O}$ ) precursor. The sample size used as the starting substrate was  $10\text{mm}\times 10\text{mm}\times 50\text{mm}$ , which was determined by a commercial organization (Metia Co., Ltd., Changwon, Korea). The samples prepared with an organic binder were dipped into the solution of inorganic precursors for periods of 0.5, 1, and 2 h at room temperature. The dipped samples were dried at  $80\text{ }^\circ\text{C}$  for a period of 1 h, and then heat treated at  $1000\text{ }^\circ\text{C}$  for a period of 1 h. In this study, drying at  $200\text{ }^\circ\text{C}$  was not carried out, compared with the conventional convert mold process. Basic formulations and experimental ranges for preparing molds by converting the organic binder to the inorganic binder are shown in Table 1. The hydrolysis reaction of the precursors used in this work was progressed with the atmospheric moisture during the dry process.

### 2.2. A new coating process

Tetraethyl orthosilicate as a  $\text{SiO}_2$  precursor, and sodium methoxide as a  $\text{Na}_2\text{O}$  precursor were used as the inorganic precursors for the new coating processes. In this work, three different coating processes were employed to fabricate the starting powders, as shown in Fig. 1. In the first process (process I), the starting particle composed of  $\text{SiO}_2$  and  $\text{Al}_2\text{O}_3$  was coated with the  $\text{Na}_2\text{O}$  precursor, and then the  $\text{Na}_2\text{O}$ -coated particle was recoated with the  $\text{SiO}_2$  precursor (Fig. 1(a)). In the second process (process II), the coating sequence of process I was inverted (Fig. 1(b)). Process III involved coating of the starting particle with a mixture of TEOS and NaOMe (Fig. 1(c)). The solution of TEOS and NaOMe mixed with 40 and 60 wt%, respectively, was stirred for 1 h at room temperature. The precursor-coated particles were dried at  $80\text{ }^\circ\text{C}$  for 1 h. The dried particles were mixed with poly(vinyl alcohol) (PVA) used as an organic binder, and formed with a pressure of 60 MPa with a cuboid shape of  $10\text{mm}\times 10\text{mm}\times 50\text{mm}$ . The prepared mold samples were heat-treated at  $1000\text{ }^\circ\text{C}$  for 1 h. Basic formulations and experimental ranges to prepare the powder and mold samples through the new coating process are shown in Table 2. The molten metal based on iron (Fe) was poured into the real mold prepared through process III with TEOS as the  $\text{SiO}_2$  precursor for thin casting.

### 2.3. Characterization and analysis

The difference before and after the chemical reactions of inorganic precursors was analyzed using a Fourier transform infrared spectrometer (FT-IR, Nicolet, Thermo Fisher Scientific, MA, USA) and an X-ray diffractometer (XRD, Philips X-pret MPD, Model PW3040, Eindhoven, Netherlands). The fracture morphology and microstructure of mold samples and starting particles were observed using a scanning electron microscope (SEM, JEOL Model JSM-5610, Tokyo, Japan), and the elemental analysis of the precursors was carried out using an energy dispersive X-ray spectrometer (EDS, energy resolution = 133 eV, Oxford Inst., Oxford, UK). The fracture strength of samples before and after the heat treatment was measured using a universal testing machine (UTM, Instron 5566, Instron Corp., Norwood, MA, USA) in the bending mode at a rate of 0.5mm·min<sup>-1</sup>. Tests were carried out at room temperature, and five runs were performed to determine the standard deviation of the strength.

Table 1. Formulations and conditions used for the mold with new inorganic precursor, and their reaction depth

Run number	Conventional binder (wt%)	TEOS (wt%)	PDMS (wt%)	NaOMe (wt%)	Isobutyl alcohol (wt%)	Dipping time (h)	Process condition	Reaction depth (mm)
1-1	100	–	–	56	6	0.5		1.49
1-2						1		2.00
1-3						2		2.57
2-1	–	38	0			0.5		3.52
2-2						1	Drying process (1 h, 80 °C)	Closed pack
2-3						2		Closed pack
3-1	–	7.6	30.4			0.5		Closed pack
3-2						1	Heat treatment (1 h, 1000 °C)	Closed pack
3-3						2		Closed pack
4-1	–	0	38			0.5		Closed pack
4-2						1		Closed pack
4-3						2		Closed pack

## 3. Results and discussion

### 3.1. The chemical reactions of inorganic precursors

Fig. 2 presents XRD profiles of the individual precursor (NaOMe and TEOS) and mixture of precursors (TEOS + NaOMe and PDMS+ NaOMe), showing materials after the hydrolysis reaction and after heat treatment under two conditions, 500 °C and 1000 °C. In Fig. 2(a), NaOMe is transformed into Na<sub>2</sub>CO<sub>3</sub> (sodium carbonate) and NaOOCH (sodium formate) via NaOH by the hydrolysis reaction. However, the NaOOCH peak completely disappeared after heat treatment at 500 °C, and Na<sub>2</sub>CO<sub>3</sub> was completely decomposed after treatment at 1000 °C. The TEOS is changed into amorphous SiO<sub>2</sub> during the hydrolysis reaction, which is very stable and independent of the heat treatment temperature (Fig. 2(b)). In the mixture of TEOS and NaOMe, the XRD result shows complex peaks of Na<sub>2</sub>CO<sub>3</sub> generated from NaOMe and amorphous SiO<sub>2</sub> from TEOS after hydrolysis (Fig. 2(c)) [12-14]. Then, these products are synthesized into the glass phase of Na<sub>2</sub>SiO<sub>3</sub> (sodium silicate) at 1000 °C via a complex mixture of Na<sub>2</sub>CO<sub>3</sub>, amorphous SiO<sub>2</sub>, and Na<sub>2</sub>SiO<sub>3</sub> under heat treatment at 500 °C. However, in the case of the PDMS without the hydrolysis reaction, results of the mixture containing PDMS and NaOMe (Fig. 2(d)) are significantly different from the results of the mixture with TEOS and NaOMe. After the hydrolysis reaction, the peak of only Na<sub>2</sub>CO<sub>3</sub> was detected. Moreover, PDMS is converted into the crystal phase of cristobalite along with complete degradation of Na<sub>2</sub>CO<sub>3</sub> during the heat treatment of 1000 °C. However, in the case of heat treatment at 500 °C, the XRD pattern shows complex peaks of Na<sub>2</sub>CO<sub>3</sub> and amorphous SiO<sub>2</sub>.



Fig. 1. Schematic diagram for fabricating the mold sample through the new coating process: (a) process I, (b) process II, and (c) process III.

Table 2. Basic formulations and experimental ranges to prepare the powder and mold samples using the new coating processes

Run number	1 <sup>st</sup> coating precursor	2 <sup>nd</sup> coating precursor	Organic binder	Condition	Fracture strength (MPa)
Run-1	-	-	-	Conventional convert mold process	4.20 ± 1.21
Run-2	NaOMe	-	-	W/o heat treatment	-
Run-3	TEOS	-	-	W/o heat treatment	-
Run-4	NaOMe	TEOS	-	W/o heat treatment	-
Run-4-1			PVA	Coating process I	6.80 ± 1.68
Run-5	TEOS	NaOMe	-	W/o heat treatment	-
Run-5-1			PVA	Coating process II	5.71 ± 0.82
Run-6	TEOS + NaOMe		-	W/o heat treatment	
Run-6-1			PVA	Coating process III	10.13 ± 0.92

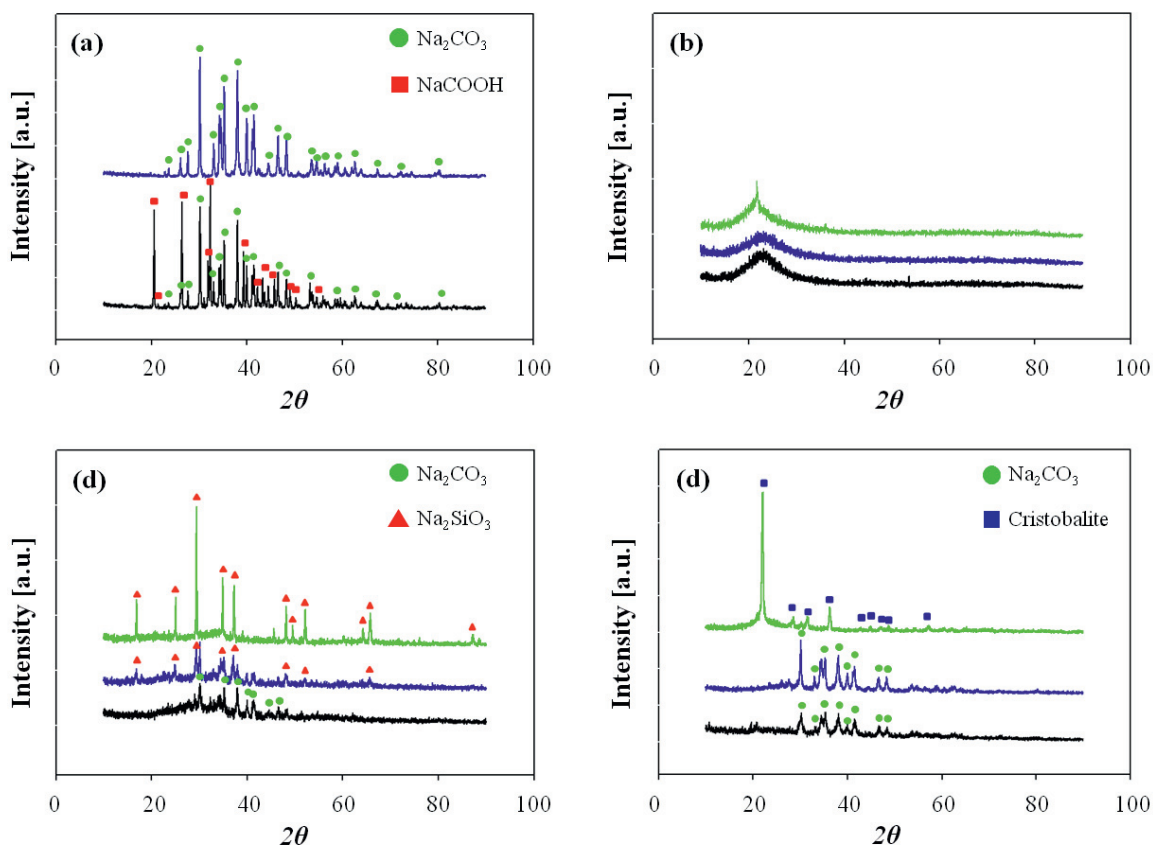


Fig. 2. XRD patterns of precursors after the hydrolysis reaction and heat treatment: (a) NaOMe, (b) TEOS, (c) mixture of TEOS and NaOMe, and (d) mixture of PDMS and NaOMe. Black, blue, and green solid lines indicate XRD patterns after hydrolysis, heat treatment at 500 °C, and heat treatment at 1000 °C, respectively [20].

FT-IR spectra of various precursor materials, such as TEOS, PDMS, and mixture materials (TEOS + NaOMe and PDMS + NaOMe) are shown in Fig. 3. Fig. 3(a) shows the products of NaOMe treated under various conditions.  $\text{Na}_2\text{CO}_3$  after the hydrolysis reaction and the heat treatment has the specific characteristic peaks of  $\text{CO}_3^{2-}$  at 1400 and 900  $\text{cm}^{-1}$ . In addition, any FT-IR peaks related to NaOMe do not appear after treatment at 1000 °C, as indicated in Fig. 3(a). In Fig. 3(b), the TEOS peak before the hydrolysis reaction shows two characteristic bands at 2800–3000  $\text{cm}^{-1}$  and 1000  $\text{cm}^{-1}$ , which are assigned to the C–H stretching vibration by the ethyl group and Si–O stretching peak, respectively. However, after the hydrolysis reaction and the heat treatment, the C–H stretching peak disappears and a peak arising from the Si–OH group occurring at 3500  $\text{cm}^{-1}$  is observed. In addition, the Si–O–Si group bending peak occurring at 470  $\text{cm}^{-1}$  is observed [15]. These results confirm that TEOS undergoes two reactions: (1) the formation of Si–OH by the hydrolysis reaction with water, and (2) a condensation reaction between Si–OH groups after the hydrolysis reaction, which is principally the sol–gel process [16–17]. In addition, the generated amorphous  $\text{SiO}_2$  does not vary under any reaction conditions (hydrolysis reaction, heat treatment at 500 and 1000 °C), as seen in Fig. 2(b). In Fig. 3(c), FT-IR spectra of the mixture with TEOS and NaOMe simply show a mixture of neat NaOMe and TEOS before the hydrolysis reaction. However, after the hydrolysis reaction and the heat treatment, it is seen that peaks arise from the  $\text{CO}_3^{2-}$ , Si–OH group, and Si–O stretching peak occurring at 1400, 3500, and 1000  $\text{cm}^{-1}$ , respectively, indicating peaks of  $\text{SiO}_2$  and  $\text{Na}_2\text{CO}_3$ . The characteristic bands arising from PDMS show an Si–OH stretching peak occurring at 3500  $\text{cm}^{-1}$ , a C–H stretching peak occurring at 2800–3000  $\text{cm}^{-1}$ , sharp and strong Si–O–Si stretching peaks occurring at 800 and 1100  $\text{cm}^{-1}$ , and an Si– $\text{CH}_3$  stretching vibration occurring at 1250  $\text{cm}^{-1}$ .

(Fig. 3(d)) [18-19]. The PDMS peaks do not change after the hydrolysis reaction. The variations before and after the hydrolysis reaction are due solely to NaOMe. This suggests that PDMS does not undergo the sol-gel reaction, resulting in a high efficiency binder system. PDMS has a molecular structure that contains Si-O-Si linkages, whereas TEOS forms these linkages after undergoing the sol-gel reaction, as shown in Fig. 3. Therefore, a significant difference in the spectra before and after the hydrolysis reaction is observed in Fig. 3(c), while a similar spectrum is shown in Fig. 3(d) except for the peak occurring at  $1600\text{ cm}^{-1}$  resulting from the NaOMe.

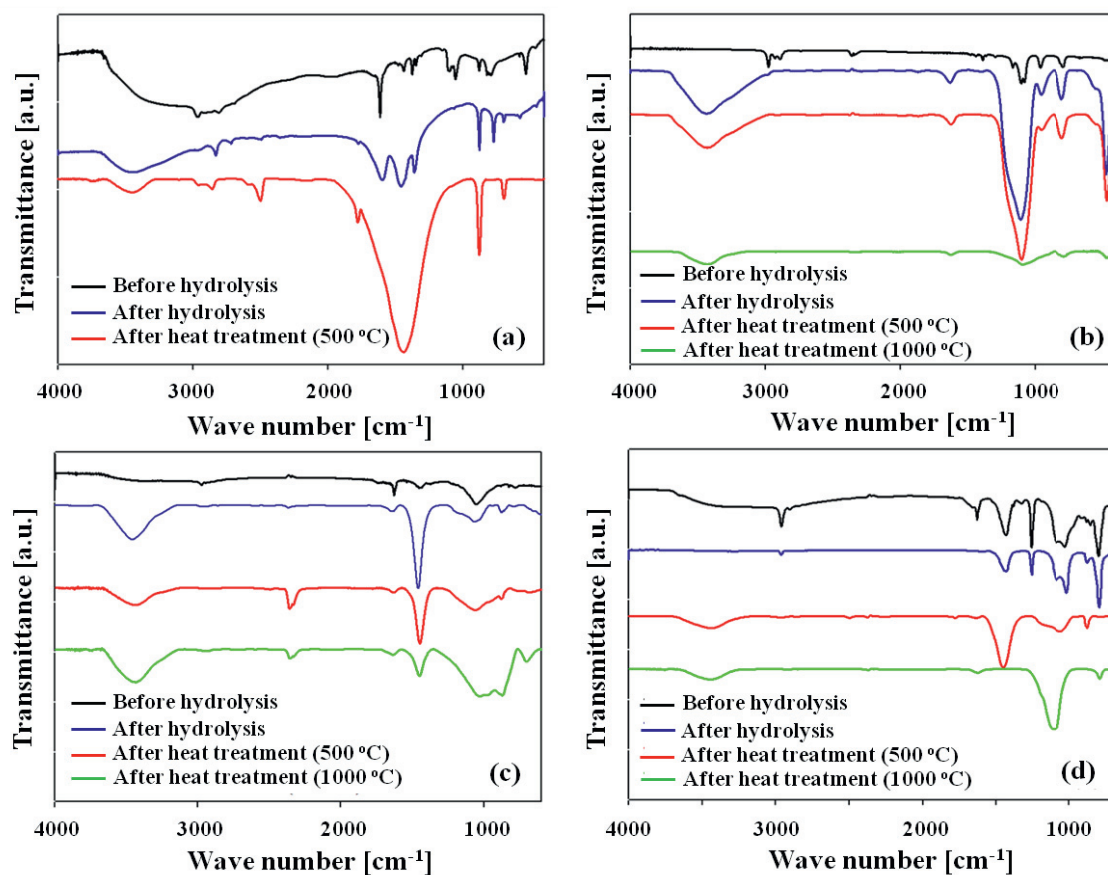


Fig. 3. FT-IR spectra of various inorganic precursors: (a) NaOMe, (b) TEOS, (c) mixture of TEOS and NaOMe, and (d) mixture of PDMS and NaOMe. Black, blue, and green solid lines imply FT-IR spectra before hydrolysis, after hydrolysis, before heat treatment at  $500\text{ }^{\circ}\text{C}$ , and after heat treatment at  $1000\text{ }^{\circ}\text{C}$  [20].

Photographs of the various precursors after the hydrolysis reaction and the heat treatment are shown in Fig. 4. NaOMe, TEOS, and the mixture of TEOS and NaOMe are transformed from a transparent liquid into white solid products after the hydrolysis reaction. However, the mixture of PDMS and NaOMe becomes a gel phase caused by the by mixing the PDMS of liquid phase and the white solid  $\text{Na}_2\text{CO}_3$  generated after the hydrolysis reaction. During the heat treatment at  $1000\text{ }^{\circ}\text{C}$ , neat  $\text{Na}_2\text{CO}_3$  is without  $\text{SiO}_2$  precursor completely degraded and the others were converted a white gel phase.

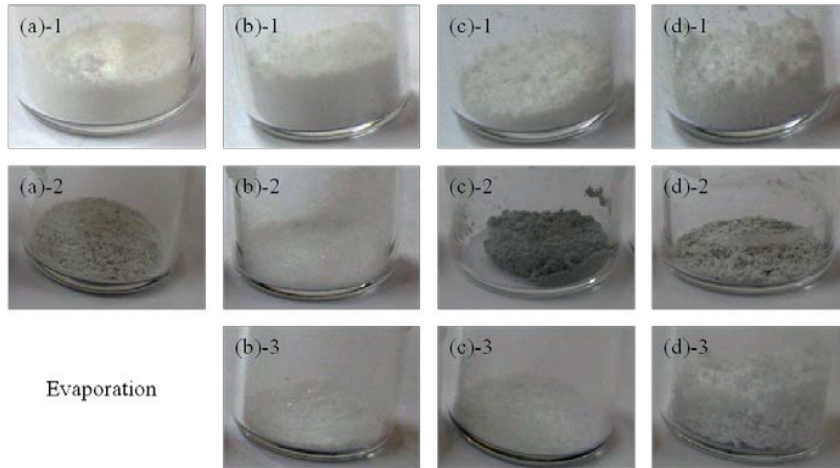


Fig. 4. Photographs of precursors after the hydrolysis reaction and the heat treatment: (a) NaOMe, (b) TEOS, (c) mixture of TEOS and NaOMe, and (d) mixture of PDMS and NaOMe. Each number means the precursor materials after the hydrolysis reaction (series 1), after the heat treatment at 500 °C (series 2), and after the heat treatment at 1000 °C (series 3) [20].

### 3.2. A new inorganic binder system

The variation of reaction depth as a function of the dipping time is shown in Table 1 and Fig. 5. The reaction depth was measured using samples dried and heat treated after dipping into the inorganic precursors prepared with a specific condition. In the case of the mold used in conventional mold process (Run 1 series), as the dipping time was increased from 0.5 to 2 h, the reaction depth of the precursors became thick from about 1.49 to 2.57 mm (see Fig. 5(a)). This means that the empty center of samples induced a significant decrease in the strength of the mold sample. However, in the new inorganic precursor systems (Runs 3 and 4 series), except for Run 2 (Fig. 5(b)), the reaction was fully built up in the whole region of mold sample during the heat treatment, indicating that the strength of mold sample may be increased. This suggests that the new inorganic precursor systems are more effective in diffusing the binder into the sample and in reducing the processing time compared with the conventional precursor system.

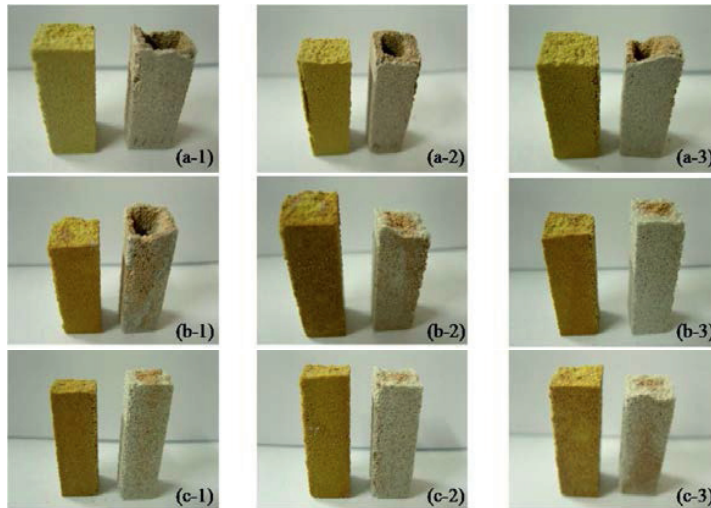


Fig. 5. Fracture morphology of mold samples before and after the heat treatment as a function of dipping time: (a) conventional precursor, (b) TEOS with NaOMe, and (c) PDMS with NaOMe. Each number indicates the dipping times of 0.5, 1, and 2 h, respectively [10].

The fracture strength of mold samples prepared with different compositions and dipping times was investigated, and the results are shown in Fig. 6. Generally, the fracture strength of samples after the heat treatment should be a higher value than that of the samples before the heat treatment due to the silicate synthesized by the reaction of  $\text{SiO}_2$  and Na ions during the heat treatment. However, in the conventional precursor system, the fracture strength decreased sharply after the heat treatment owing to the large hole created inside the sample by non-reacted precursors. However, in the case of the precursors containing PDMS (Runs 3 and 4), the fracture strength after the heat treatment was significantly increased compared with the conventional precursor system, caused by the high glassification efficiency of PDMS without the sol-gel process and by the relatively deep reaction depth. Except for the conventional precursor system, the fracture strength decreased slightly as the dipping time increased due to agglomeration and reverse diffusion. The new inorganic precursor system with 7.6 wt% PDMS (Run 3-1) showed the highest nominal strength of 8 MPa, meaning the excess additional PDMS did not affect the fracture strength.

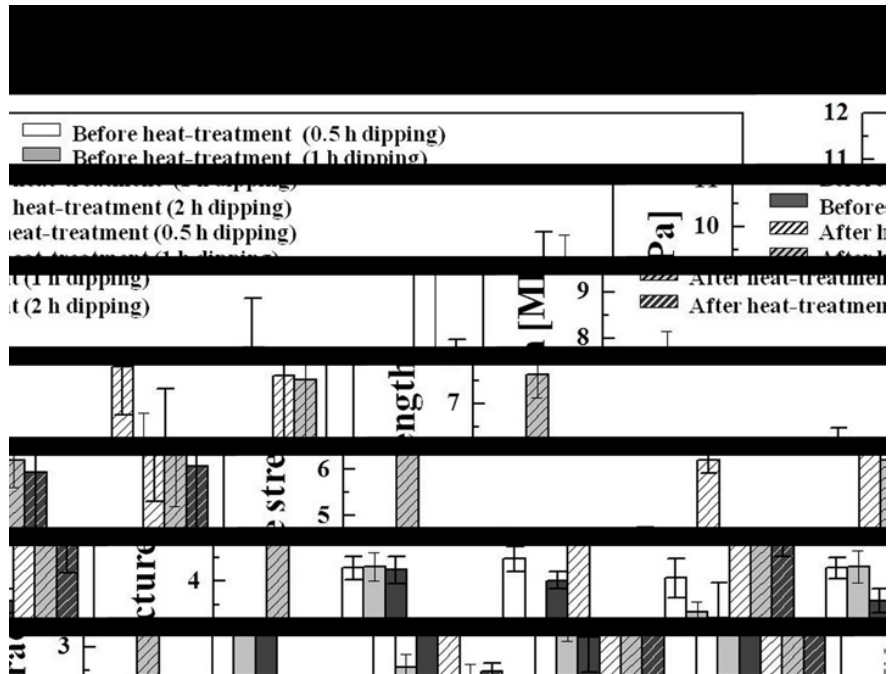


Fig. 6. Fracture strength of mold samples before and after the heat treatment as a function of dipping time. Each number indicates binder species of conventional precursor, TEOS with NaOMe, TEOS (7.6 wt% PDMS) with NaOMe, and PDMS with NaOMe, respectively [10].

As shown in Fig. 7, the glass phase was well developed at the interface (Fig. 7(c)) and/or on the surface (Fig. 7(d)) of starting particles prepared by the precursors containing PDMS (indicated with arrows in Fig. 7), while the glass phase was not fully developed at the particles prepared by the precursors without PDMS, especially in the case of conventional precursor system (Fig. 7(a)). It means that precursor of siloxane type without the sol-gel reaction has a higher glassification efficiency than that of silicate type with the hydrolysis and condensation reactions, showing the higher strength in mold samples prepared by the new precursor system containing PDMS.

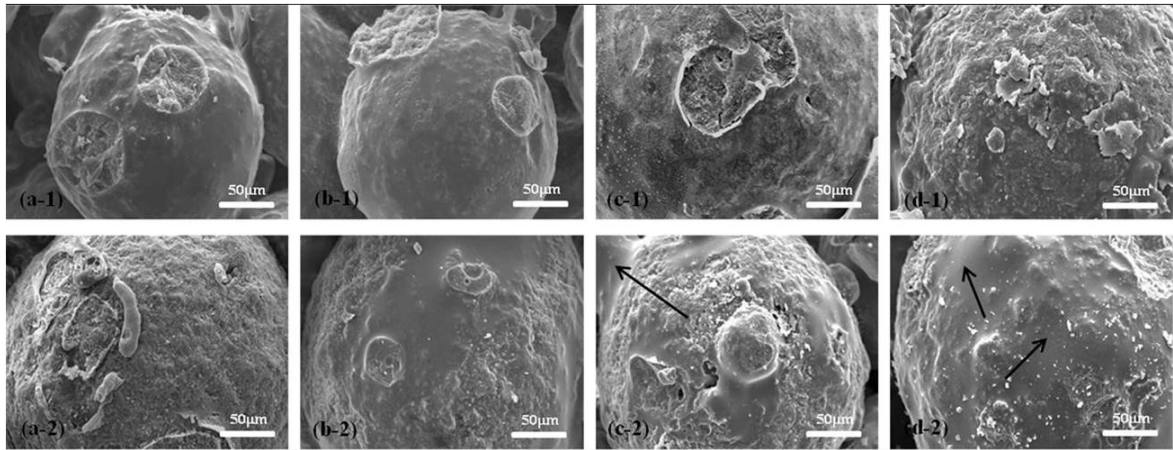


Fig. 7. SEM morphology of particles in the fracture surfaces of samples prepared with dipping time of 2 h before and after the heat treatment as a function of composition: (a) conventional precursor, (b) TEOS with NaOMe, (c) TEOS (7.6 wt% PDMS) with NaOMe, and (d) PDMS with NaOMe. Arrows indicate the glass phases formed at the interface and on the surface of particles in mold samples prepared by the precursor systems containing PDMS after the heat treatment [10].

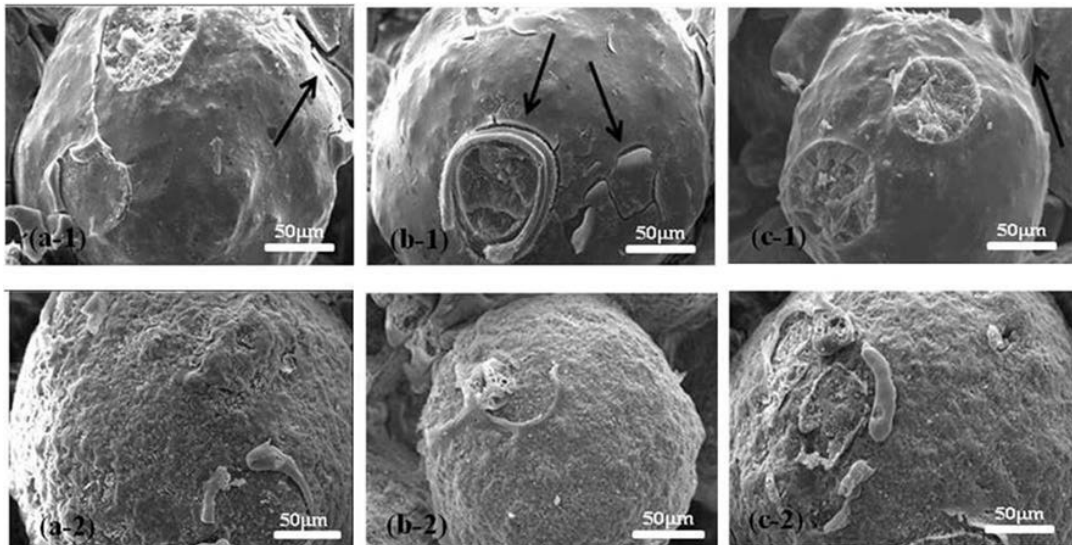


Fig. 8. SEM morphology of particles in the fracture surfaces of samples prepared by Run 2 before and after the heat treatment as a function of dipping time: (a) 0.5 h, (b) 1 h, and (c) 2 h. Each number indicates morphologies before and after the heat treatment, respectively. Arrows indicate cracks formed at the interface and on the surface of particles [10].

Typical SEM morphologies of particles in the fracture surfaces of mold samples prepared by Run 2 before and after the heat treatment are shown in Fig. 8 as a function of dipping time. Before the heat treatment, cracks were observed at the interface between particles (denoted by the arrows in Fig. 8(a-1) and (c-1)), and on the surface of particles (denoted by the arrow in Fig. 8(b-1)), whereas these cracks disappeared after the heat treatment due to the formation of the glass phase. All particles were well coated by the inorganic precursors, regardless of the dipping time.

### 3.2. A new coating process

Typical cross-sectional morphologies of the particles treated under various conditions are presented in Fig. 9, which are observed in the particles after the hydrolysis or sol–gel reactions following the drying process. As mentioned above, the particle with the NaOH generated by the hydrolysis reaction of NaOMe represent the particulate layer with a polygonal shape (denoted by the dotted arrows in Fig. 9(a)), while the particle with the SiO<sub>2</sub> by the sol–gel reaction of TEOS shows the layer with a continuous solid state on the surface of the starting particle (denoted by the solid arrows in Fig. 9(b)). In the SEM image of the particle prepared through process I (Fig. 9(c)), the layers of SiO<sub>2</sub> and NaOH are not independently observed on the surface of the starting particle, meaning that TEOS has permeated between the NaOH particles. Therefore, it can be assumed that a single layer with a mixture of SiO<sub>2</sub> and NaOH phases is formed. However, in the case of Fig. 9(d), the layers of SiO<sub>2</sub> and NaOH are observed on the surface of the particle, indicated by the solid and dotted arrows, respectively. This is because the continuous glass state of SiO<sub>2</sub> restricts the infiltration of NaOMe.

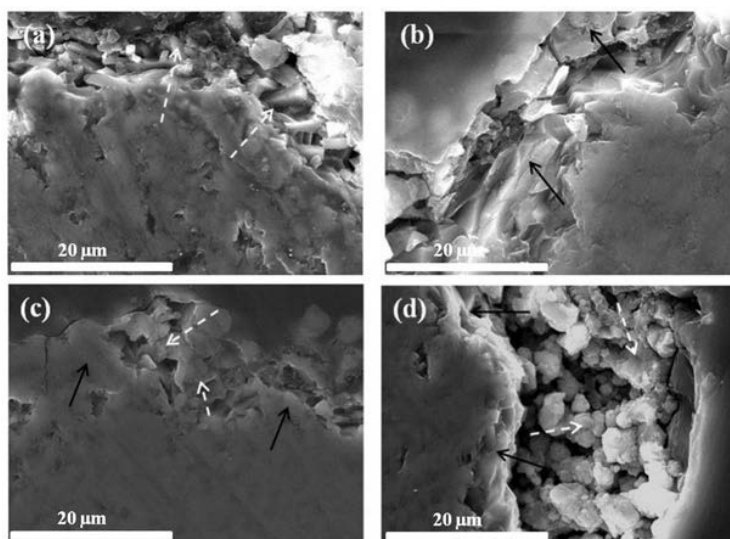


Fig. 9. SEM morphologies of the particles coated with inorganic precursors: (a) NaOMe, (b) TEOS, (c) process I, and (d) process II. White and black arrows indicate the NaOH and SiO<sub>2</sub> phases, respectively [11].

These phenomena can be confirmed in the element analysis results for the particles prepared through each coating process, presented in Fig. 10. The starting particle used in this work is mostly composed of SiO<sub>2</sub> and Al<sub>2</sub>O<sub>3</sub>, with Al and Si elements homogeneously dispersed on the surface of the particle. In Figs. 10(a-2) and (a-4), the Na and Si are uniformly observed on the surface of the particle because of the mixture of SiO<sub>2</sub> and NaOH, as mentioned in the SEM morphology. However, in the case of Fig. 10(b-2), a considerable amount of Na is detected on the outside of the particle, meaning that the phases of SiO<sub>2</sub> and NaOH exist separately, compared with the particle treated by process I. It could be expected that the mold prepared through process I has a higher fracture strength than that prepared by process II, caused by the improvement in the glassification efficiency because of the homogeneous mixing between the SiO<sub>2</sub> and NaOH phases at the surface of the particle.

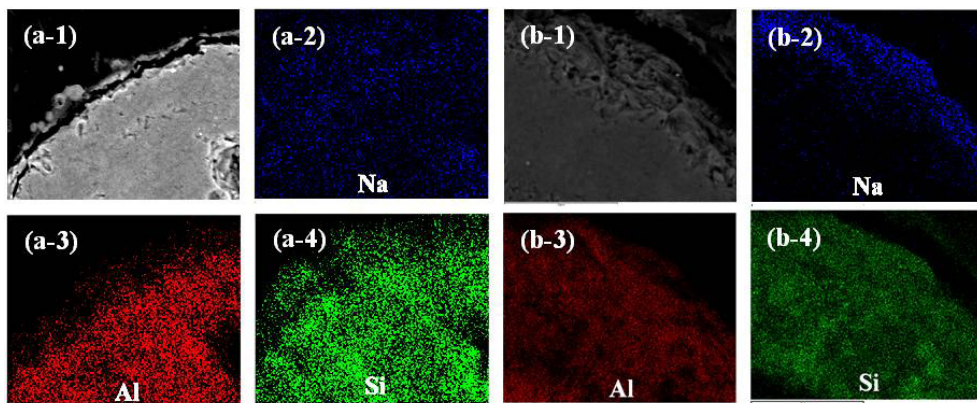


Fig. 10. Element analysis results of the particles prepared through process I (a) and process II (b). Each number presents SEM morphology of particle, and elements of Na, Al, and Si, respectively [11].

Typical cross-sectional morphologies and the element analysis results of the particles prepared through process III before heat treatment are shown in Figs. 11 and 12, respectively. The TEOS of the continuous solid state and the NaOMe of the particulates are homogeneously mixed and then coated on the surface of the starting particle (Fig. 11), resulting in the Na and Si are uniformly observed on the surface of the particle (Fig. 12).

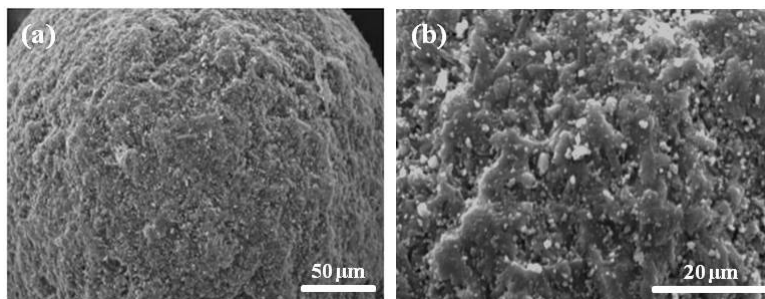


Fig. 11. SEM morphology of the particle prepared through process III before heat treatment: (a) low magnification and (b) high magnification [11].

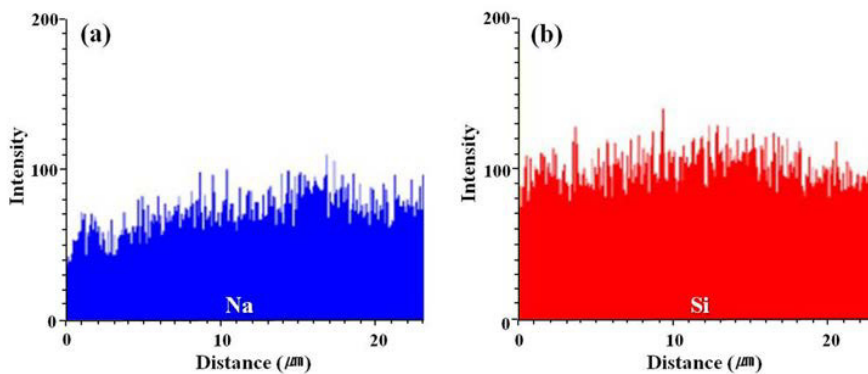


Fig. 12. Element analysis results of the particle prepared through process III before heat treatment: (a) Na element and (b) Si element [11].

Surface morphologies of the mold prepared as a function of process are shown in Fig. 13. The glass phase is observed at the interface between particles and on the surface of particles, independent of the process. The particle prepared by the conventional convert mold process shows a less homogeneous glass phase (indicated by the solid arrow in Fig. 13(a)), compared with those by the new coating processes, caused by the loss of inorganic precursors by the decomposition of organic binder during the heat treatment. In the mold prepared by process III, the glass phase is the most homogeneously dispersed at the interface between particles and on the surface of the particles, as shown in Fig. 13(d), resulting from the high glassification efficiency by the homogeneous mixture of each inorganic precursor. In addition, in process I, the glass phase is well and uniformly developed because of the increase in the contact area between  $\text{SiO}_2$  and  $\text{NaOH}$  existing simultaneously in the mixture layer, as shown in Fig. 13(b). However, in Fig. 13(c), the glass phase of sodium silicate is locally and partially seen on the surface of the particles. In the case of process II, the glassification is reduced because of the low reaction between the  $\text{SiO}_2$  and  $\text{NaOH}$  molecules being in the double layer as well as the evaporation of elemental Na present at the outside of the particle. It is verified that the Na strongly affects the generation of glass phase, showing the higher strength in the mold prepared by process I than by process II.

Fig. 14 shows photographs of the mold prepared through process III. Two solid phases ( $\text{SiO}_2$  and  $\text{NaOH}$ ) generated by hydrolysis and/or condensation reactions (see Fig. 14(a)) are converted into the glass phase of sodium silicate ( $\text{Na}_2\text{SiO}_3$ ) during the heat treatment, having a white solid phase, as shown in Fig. 14(b).

The fracture strengths of molds prepared through each process were measured at room temperature, and the results are shown in Table 1. The new coating processes introduced in this work are designed to decrease the loss of inorganic precursors by the coating of organic binder onto the inorganic precursors. It induces the enhancement of glassification efficiency of the precursor. Therefore, the fracture strengths in mold samples prepared by the new processes are significantly increased compared with that of the conventional convert mold process. In addition, the fracture strength value of the mold sample prepared by process III is higher than those of processes I and II because of the high glassification efficiency and the uniform glassification by the high mixing effect between precursors.

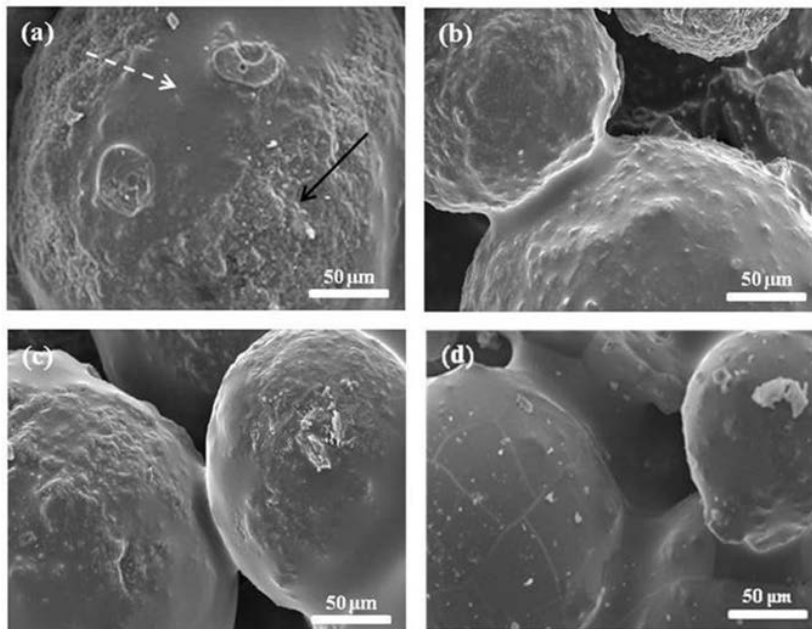


Fig. 13. SEM morphologies of particles after heat treatment in mold samples prepared by (a) conventional mold process, (b) process I, (c) process II, and (d) process III [11].

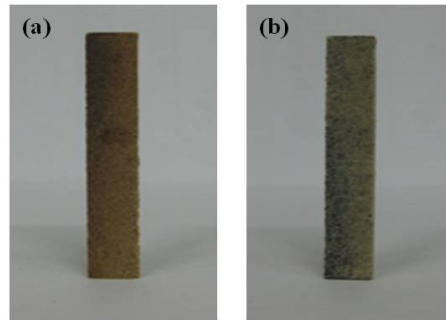


Fig. 14. Photographs of the mold samples prepared through process III: (a) before heat treatment and (b) after heat treatment. Photograph of each sample is real size of 10mm×10mm×50mm [11].

#### 4. Conclusions

A new inorganic precursor and a new process have been developed and introduced to homogeneously form of glass phase on the interfaces and surfaces of starting particles as well as the enhancement of coating and glassification efficiencies of inorganic precursors, for preparing the mold with high strength of mold for thin-wall casting.

The new inorganic precursor systems were successfully developed using precursor materials, such as tetraethyl orthosilicate (TEOS), polydimethyl siloxane (PDMS), and sodium methoxide (NaOMe). TEOS was converted into silica ( $\text{SiO}_2$ ) by a sol–gel process, whereas PDMS did not undergo any chemical reaction, highlighting the difference between PDMS and TEOS in terms of the final fracture strength. The fracture strength of mold samples with the new inorganic precursor mostly increased after the heat treatment due to the increase in glassification and the relatively narrow reaction depth. In addition, the new binder system with 7.6 wt% PDMS showed the highest nominal strength of 8MPa, due to the high glassification efficiency of PDMS without the hydrolysis and condensation reactions. The SEM morphology of particles was independent of the dipping time, but the composition significantly affected the glassification.

A new coating process has been introduced to enhance the coating effect of inorganic precursors, related to the coating of inorganic precursor prior to organic binder on the starting particles, compared with the conventional mold process. It induces the homogeneous formation of the glass phase on the surface of starting particle and the increase in the glassification efficiency of inorganic precursor. Namely, the new coating process significantly reduces the loss of inorganic precursors by burning of organic binder occurred in the conventional mold process, leading to an improvement in the fracture strength of mold. In the surface morphology of the particles prepared by process III, the glass phase is well and uniformly formed both at the interface between particles and on the surface of the particles. This is because of the increase in the glassification efficiency by the high reactivity between  $\text{SiO}_2$  and NaOH. However, the glass phase generated under process II is locally and partially generated on the surface of the particles in the mold, probably related to the evaporation of elemental Na presented at the outside of the mold and the low reactivity between the two inorganic precursors. Therefore, the fracture strength of the mold sample prepared by process III is higher than those prepared by processes I and II, whereas the conventional convert mold process results in the lowest fracture strength, indicating that the new coating process can provide a high strength mold.

#### Acknowledgements

This work was supported by the National Research Foundation of Korea (NRF) grant funded by the Korean Government (MSIP) (No. 2011-0030058), by a grant from Fundamental R&D Program for Core Technology of Materials funded by the Ministry of Knowledge Economy (10041233), and by the Technology Innovation Program (10043795, Development of Materials for Gas Turbine Operated at 1600 °C for High-Efficiency Power Generation) funded by the Ministry of Knowledge Economy (MKE).

## References

- [1] Y.A. Meng, B.G. Thomas, *Metall. Mater. Trans.* 34B (2003) 707.
- [2] M. Şimşir, L.C. Kumruoğlu, A. Özer, *Mater. Designs* 30 (2009) 264.
- [3] H. Saridikmen, N. Kuskonmaz, *Ceram. Int.* 31 (2005) 873.
- [4] J. Jiang, X.Y. Liu, *Mater. Process Technol.* 189 (2007) 247.
- [5] M.W. Barsoum, *Fundamentals of Ceramics*, McGraw-Hill, Seoul, 1997.
- [6] W.D. Callister, *Materials Science and Engineering: An Introduction*, Wiley, New York, 1997.
- [7] S. Ege, *Organic Chemistry*, D.C. Heath and Company, Toronto, 1994.
- [8] P.G. Shewmon, *Diffusion in Solids*, McGraw-Hill, New York, 1963.
- [9] N. Sasaki, *Found. Manage. Technol. (Feb.)* (2009) 21.
- [10] E.H. Kim, W.R.Lee, Y.G. Jung, C.S.Lee, *Materials Chemistry and Physics* 126 (2011) 344.
- [11] E.H. Kim, G.H. Jo, J.H. Lee, Y.G. Jung, J. Ha, U. Paik, *Ceramics International* 38 (2012) 2749.
- [12] X. Shi, S. Xu, J. Lin, S. Feng, J. Wang, *Mater. Lett.* 63 (2009) 527.
- [13] Y. Chen, Y. Hong, F. Zheng, J. Li, Y. Wu, L. Li, *J. Alloys Compd.* 478 (2009) 411.
- [14] J.L. Gurav, A.V. Rao, A.P. Rao, D.Y. Nadargi, S.D. Bhagat, *J. Alloys Compd.* 476 (2009) 397.
- [15] M. Anbia, M. Lashgari, *Chem. Eng. J.* 150 (2009) 555.
- [16] W. Xue, A. Bandyopahyay, S. Bose, *Acta Biomater.* 5 (2009) 1686.
- [17] G.F. Terry Lay, M.C. Rockwell, J.C. Wiltshire, C. Ketata, *Ceram. Int.* 35 (2009)1961.
- [18] P.K. Sahoo, R. Samal, S.K. Swain, P.K. Rana, *Eur. Polym. J.* 44 (2008) 3522.
- [19] A.K. Sandhu, W. Singh, O.P. Pandey, *Mater. Chem. Phys.* 115 (2009) 783.
- [20] E.H. Kim, J.H. Lee, C.S.Lee, Y.G. Jung, *Journal of the European Ceramic Society* 31 (2011) .